Paper V

Dagestad, K-F. (2005)

Simulations of bidirectional reflectance of clouds with a 3D radiative transfer model

Manuscript

Simulations of bidirectional reflectance of clouds with a 3D radiative transfer model

Knut-Frode Dagestad
Geophysical institute
University of Bergen, Norway
May 2005

Abstract

To get an impression of the impact of the hetereogeneity of cloud properties on the radiance observed by a satellite for various pixel sizes, a 3-dimensional radiative transfer model (SHDOM) is used to simulate radiances reflected to space from two cloud fields. For a given sun-cloud-satellite geometry and for a typical stratocumulus cloud field the radiance is mainly unaffected by rotating the cloud in the azimuth direction when the pixel size is 3.5 kilometres. For a pixel size of 550 metres there is some more variability, and for a pixel of 55 metres the variability of the radiance is larger than 100%. As expected, the variability is much larger for a typical cumulus cloud than for the stratocumulus field. Even for a field as large as 6.7 kilometres there is some variability in the radiance by rotating the cloud field. For pixels of 670 metres or smaller the variability is extreme, as clouds are obstructing the viewing path for some rotations and not for others. The angular distribution of simulated radiances from the stratocumulus field is also compared to reflectances measured with the Meteosat High Resolution Visible sensor. The angular distribution of the simulated radiances is similar to what is observed by Meteosat for thin clouds. For the thicker clouds the distribution of Meteosat reflectances is closer to lambertian.

1 Introduction

For many purposes it is useful to have a description of the fraction of solar radiation that clouds reflect in different directions. However, a general function can never be found, as the variable 3-dimensional structure of clouds makes the reflectance literally unpredictable.

The Heliosat-algorithm (e.g. Cano et al. 1986, Beyer et al. 1996, Fontoynont et al. 1998, Rigollier et al. 2004) estimates global irradiance from satellite images by a two step process:

- first, the combined reflectance from both ground and clouds, measured by the high resolution visible sensor, is used to calculate the "cloud index", a single parameter describing the cloud cover.
- second, this cloud index is combined with a clear sky model to estimate the actual global irradiance at ground.

This study addresses one of the implicit assumptions in this approach: that a cloud field is uniquely determined by its reflectance in one particular direction. A 3-dimensional radiative transfer model, SHDOM, will be used to assess the variability related to this assumption. SHDOM is used to simulate the reflected radiances in different directions from two different cloud fields. One of the cloud fields is a rather homogenous stratocumulus field, while the second is a broken cumulus field. Keeping the sun-ground-satellite geometry (and everything else) constant, the cloud fields are rotated 0, 90, 180, and 270 degrees in the azimuth direction. So, with the cloud properties constant (except for the rotation) the variability of the reflectance, and hence the cloud index, will be investigated. Finally the spatial distribution of reflectance will be compared with actual reflectances (though normalised) from the High Resolution Visible sensor of the Meteosat satellite.

2 The 3D radiative transfer model SHDOM

SHDOM is an acronym for "The Spherical Harmonics Discrete Ordinate Method" for three-dimensional atmospheric radiative transfer, and it is developed by Frank Evans (Evans 1998). The code combines both discrete ordinates and spherical harmonics to solve the radiative transfer equation. Spherical harmonics are used to compute the source functions and the scattering integral. This method saves a lot of computer memory, since in practice the source function is often zero or smooth for large parts of the medium, and hence can be represented with few spherical harmonic terms. Another advantage is that the scattering integral is more efficiently computed in spherical harmonics than in discrete ordinates. Discrete ordinates are used to compute the radiance field, which is then used to compute the source function, and the process repeats until a stable solution is found. To speed up calculations and to save memory an adaptive grid is used; i.e. the model can start with a rather coarse grid, and fills inn extra grid points for better accuracy whenever gradients exceed a certain threshold. 3D radiative transfer calculations consume a lot of computer memory compared to 1D calculations, so the methods used to save memory makes it possible to have cloud fields with adequate spatial resolution even with 1 GB of memory. The model is not restricted to only atmospheric calculations; the input medium can be specified completely generally with extinction, single scattering albedo, scattering phase function and temperature. The simulations are done for non-polarized and monochromatic radiation, but the correlated k-distribution method can subsequently be used for integration over a spectral band. The horizontal boundaries of the input/output field may be specified as open or periodic, and the latter is used for the simulations in this paper.

3 Input data

Two cloud fields are used as input to SHDOM:

- An overcast stratocumulus field obtained from a Large Eddy Simulation from the 1987 FIRE experiment (Moeng et al. 1996)
- A broken cumulus cloud field, reconstructed from a Landsat image by Frank Evans, the author of SHDOM

Both cloud fields were used in the second round of the Intercomparison of 3D Radiation Codes, I3RC (http://i3rc.gsfc.nasa.gov/cases_new.html). Each grid point of the cloud fields contains a droplet effective radius in micrometres and a Liquid Water Content (LWC) in grams of liquid water per cubic metres. For the runs with SHDOM a gamma distribution with a shape parameter of 7.5 was used for the droplet size distribution. The cloud fields were then combined with a Mie scattering table for the wavelength of 670 nanometres to specify the extinction, single scattering albedo and phase function at each grid point. Table 1 shows technical data of the two cloud fields, and Figures 1a and 1b and show the vertical Liquid Water Path (LWP). There were no aerosols in the atmosphere, and the ground albedo was set to zero.

Table 1: Technical data about the two cloud fields input to SHDOM

	Stratocumulus	***Cumulus***
Horizontal pixel size [m]	55	67
Number of pixels horizontally	64	100
Number of pixels vertically	16	36
Total horizontal size [m]	3520	6700

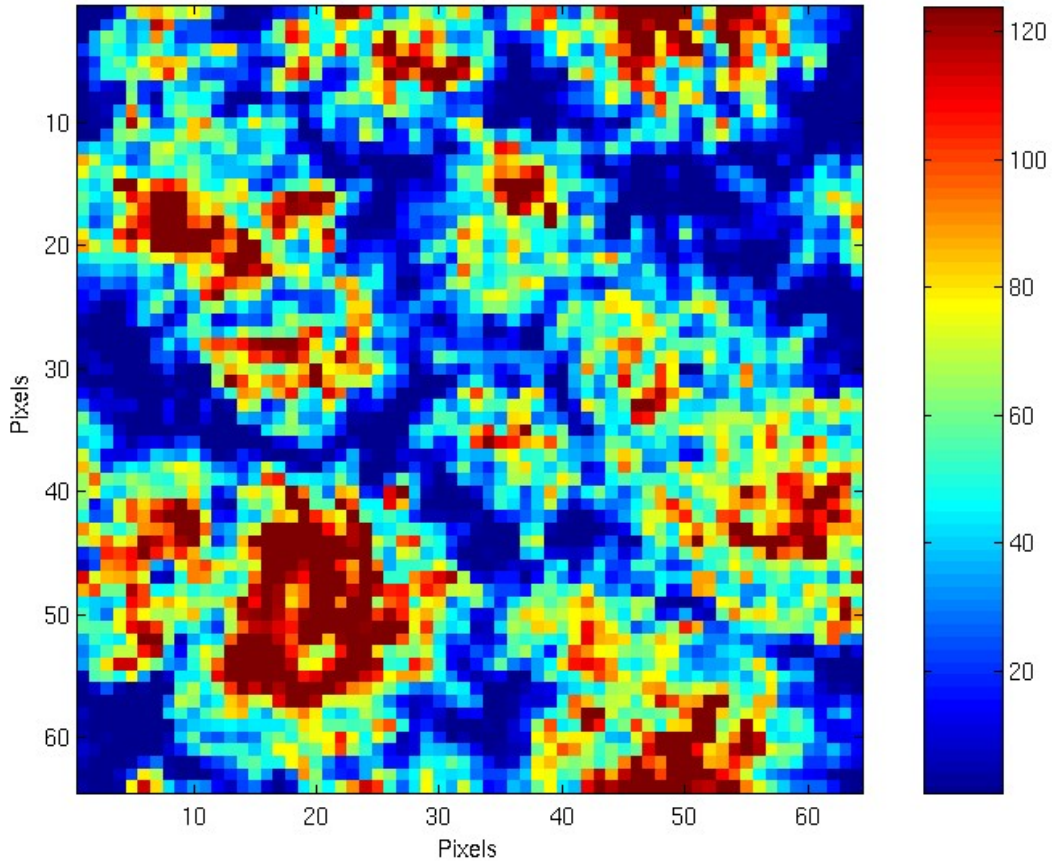

Figure 1a: Vertically integrated liquid water content (g/m^2) for the stratocumulus cloud field.

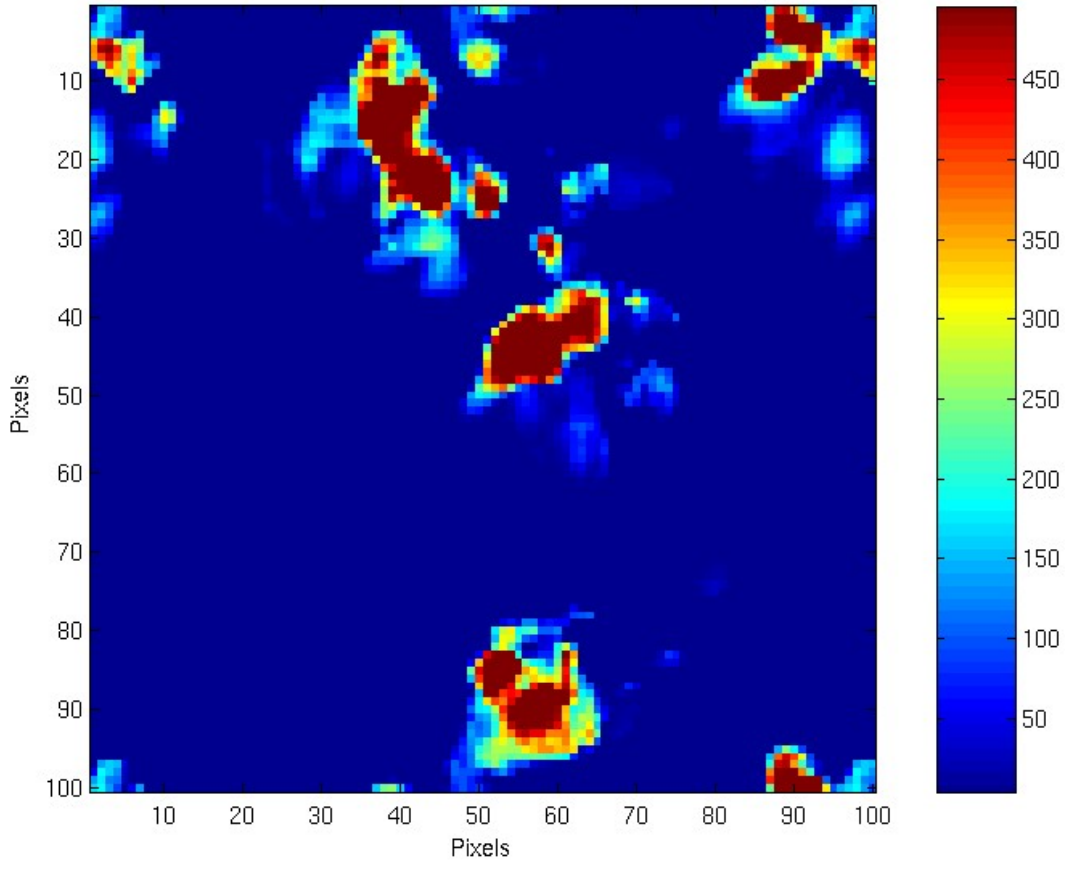

Figure 1b: Vertically integrated liquid water content (g/m^2) for the cumulus cloud field.

4 Results

Two slightly different experiments are performed:

- In section 4.1 the variability of the reflectances from two cloud fields is investigated by rotating the cloud fields while keeping everything else constant. This will be done for different sizes of the observed area of the cloud field. Thus, this will show to what extent the 3-dimensional inhomogeneities of the clouds affect radiances observed by a satellite sensor, and the pixel size needed to minimise the variability.
- In section 4.2 the variation of the bidirectional reflectance with the sun-cloud-satellite geometry is analysed. Here, simulations with an overcast stratocumulus cloud field are compared with reflectances observed with Meteosat.

4.1 Variability of simulated radiances

4.1.1 Experimental setup

3D simulations consume much more computer power than 1-dimensional models, so only some case studies were performed with SHDOM. The simulated radiances are monochromatic at the wavelength 670 nanometres. For each cloud field upward radiances were calculated for the following configurations:

- The cloud field was rotated 0, 90, 180 and 270 degrees in the azimuth direction
- Six different solar zenith angles were used: 0, 30, 60, 70, 80 and 85 degrees
- For each rotation of the cloud field and each solar zenith angle, radiances were calculated for three different viewing (satellite) zenith angles: 45, 70 and 80 degrees. The view azimuth angle was always the same as the solar azimuth angle.
- Radiances were averaged over three different subsets of the actual cloud fields:

  - The pixel in the middle of the cloud field
  - 10x10 pixels in the middle of the cloud field
  - The whole cloud field

  This corresponds to "satellite pixel sizes" of 55, 550 and 3520 metres, respectively, for the stratocumulus field and 67, 670 and 6700 metres, respectively, for the cumulus field (Table 1).

The experiment is performed to quantify the variation of the observed radiance for different "satellite pixels sizes" when the cloud field is rotated. Since the cloud fields remain unchanged the rotation should then isolate the effect of heterogeneity from other cloud properties.

4.1.2 The stratocumulus cloud field

The upper part of Figure 2 shows the simulated radiances from the stratocumulus cloud field with a view zenith angle of 45 degrees. It is seen that the radiance integrated over the whole cloud field is practically independent of the rotation of the cloud field. A noticeable variability of the radiance is seen for the 10 times 10 pixel subset and for the single pixel the radiance is varying by more than 100 percent. For all subsets a significant decrease of the reflectance is seen when the solar zenith angle is larger than 60 degrees. An explanation for this could be that the "bumps" on the top of the cloud field is scattering a large fraction of the radiation close to the forward direction, which is characteristic of Mie scattering. Thus a large part of this radiance can escape the cloud field with only a single or few scattering events.

The results for a view zenith angle of 70 degrees are seen on the lower part of Figure 2. The

radiance from the whole cloud field is still unaffected by the rotation of the cloud field. For the smaller subsets there is a somewhat smaller variability than for a view zenith angle of 45 degrees, both in relative and absolute differences. An exception is for solar zenith angles larger than 60 degrees, where the variability for the subsets is similar for both view zenith angles. For a view zenith angle of 70 degrees a peak in the reflectance is seen when the solar zenith angle is close to the view zenith angle. This is the opposition effect: no shadows are seen when the sun and the observer is in the same direction, and the cloud looks brighter. This effect is not clearly seen for the view zenith angle of 45 degrees (upper part of Figure 2).

The results from a view zenith angle of 80 degrees are very similar to the case with view zenith angle of 70 degrees, and the results are therefore not shown.

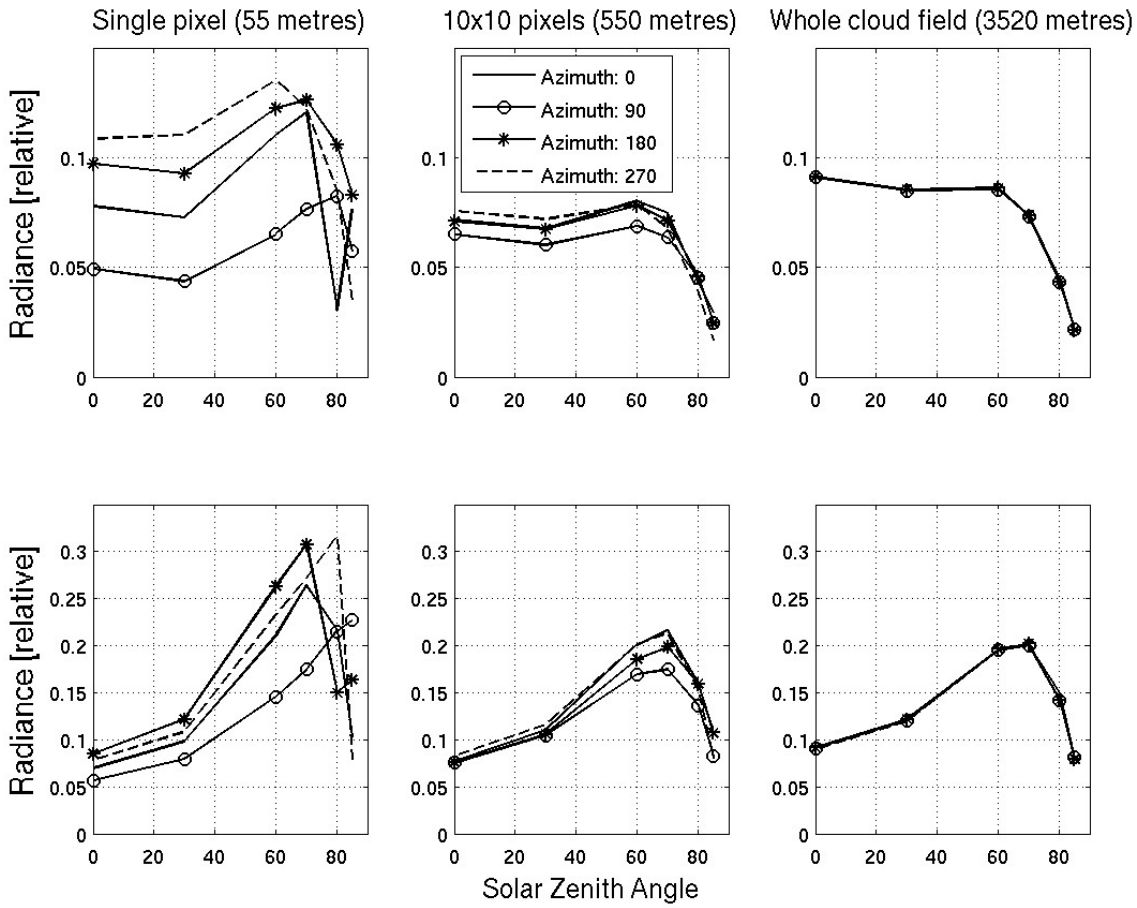

Figure 2: Simulated radiances from the stratocumulus cloud field for view zenith angles of 45 degrees (upper part) and 70 degrees (lower part) plotted versus the solar zenith angle. The left figures show the mean radiance from a single pixel in the middle of the cloud fields, the middle figures are for a subset of 10x10 pixels in the middle of the cloud field, and the rightmost figures show the mean radiance from the whole cloud field (64x64 pixels). The different lines are the radiances after rotating the cloud field 0, 90, 180 and 270 degrees in the azimuth direction. The incoming irradiance on a horizontal plane at the top of the atmosphere is one unit. The view azimuth angle is always the same as the solar azimuth angle. Note different scale on y-axes for upper and lower part.

4.1.3 The cumulus cloud field

Radiances from the cumulus cloud field with a view zenith angle of 45 degrees are shown on the upper part of Figure 3. As expected, the variability is larger than for the stratocumulus field. Even the mean radiance from the whole cloud field (6700x6700 metres) shows some, although not dramatic, variability from the rotation. However, for the smaller subsets, the variability is very large, with observed radiances close to zero for some of the rotations. Although the same pixels at

the top of the cloud field are viewed from above, the path to the ground is obstructed by clouds at a lower level for to of the rotations, while the path is clear for the others.

For a view zenith angle of 70 degrees the results are similar (lower part of Figure 3). But for the cumulus cloud field no clear opposition effect like in Figure 2 is observed. The reason is probably that there are very little shadows on the scattered clouds in the cumulus field.

The large decrease of radiance for solar zenith angle above 60 degrees, which is observed for the stratocumulus field, is not seen for the cumulus field. Since the cumulus clouds are thicker than the "bumps" on top of the stratocumulus field, radiation penetrating the clouds probably encounters multiple scattering events, also when the radiation is coming from a very high solar zenith angle. Thus, fewer photons escape in the forward direction for low sun with the cumulus field than with the stratocumulus field. Like for the stratocumulus cloud field the results for a view zenith angle of 80 degrees are similar to those for a view zenith angle of 70 degrees, and hence these results are not shown.

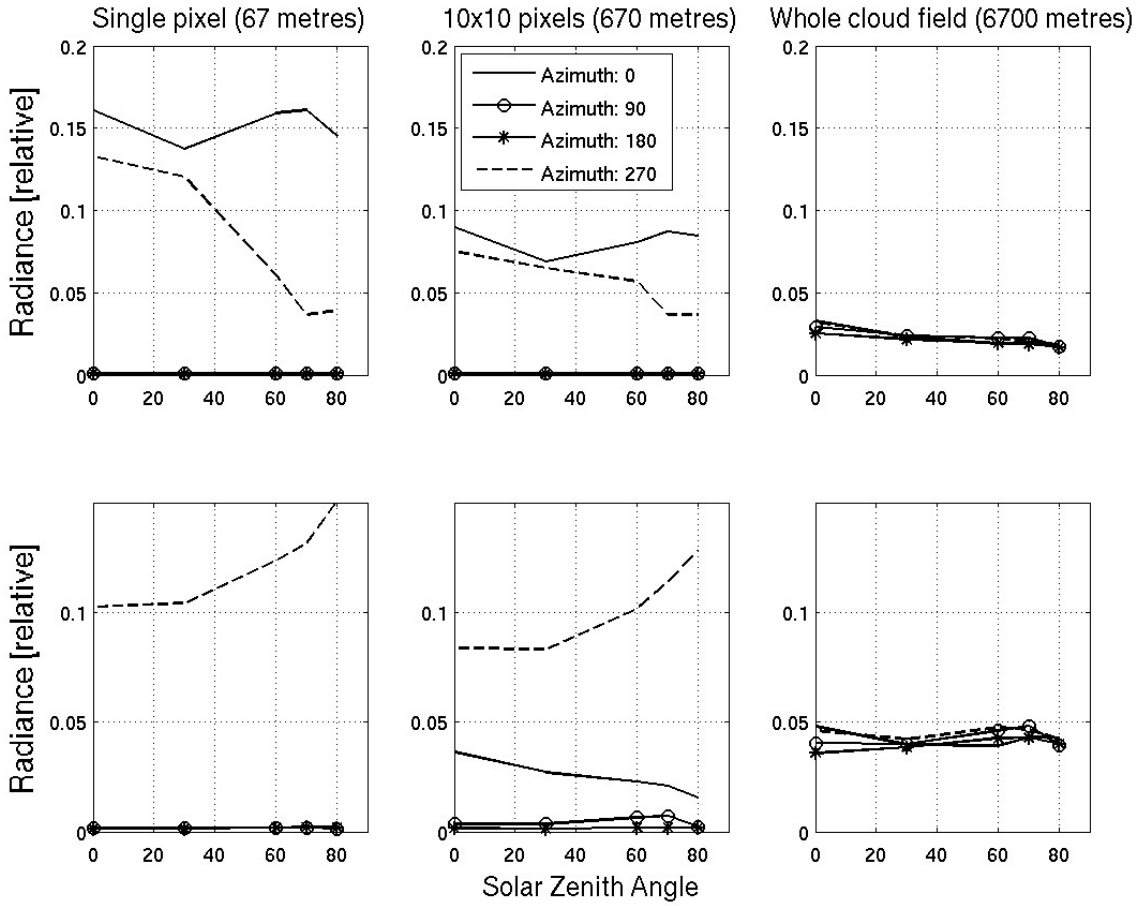

Figure 3: Simulated radiances from the cumulus cloud field for view zenith angles of 45 degrees (upper part) and 70 degrees (lower part) plotted versus the solar zenith angle. The left figures show the mean radiance from a single pixel in the middle of the cloud fields, the middle figures are for a subset of 10x10 pixels in the middle of the cloud field, and the rightmost figures show the mean radiance from the whole cloud field (100x100 pixels). The different lines are the radiances after rotating the cloud field 0, 90, 180 and 270 degrees in the azimuth direction. The incoming irradiance on a horizontal plane at the top of the atmosphere is one unit. The view azimuth angle is always the same as the solar azimuth angle. Note different scale on y-axes for upper and lower part.

4.2 Comparison with bidirectional reflectance from Meteosat

In this section the reflected radiances simulated with SHDOM are compared to measurements from the High Resolution Visible (HRV) sensor of the Meteosat satellite. A description of the full 3-dimensional distribution of reflectances is difficult, so a single angular parameter will be used for this purpose. The angle between the directions towards the sun and the satellite as seen from the cloud ("co-scattering angle", ψ) is convenient; the scattering phase function of cloud droplets depend solely on this angle, and besides this is the single parameter best describing the amount of shadows seen on a rough surface.

4.2.1 Bidirectional reflectance observed with the Meteosat HRV sensor

Pixel counts from Meteosat-5 for all images in 1996 have been extracted for the 61 locations shown on Figure 4. This amounts in total to 425711 values. The HRV channel of Meteosat has a spectral response function from 0.45 to 1.0 micrometres and so responds to visible and near infrared radiation. The raw pixel counts, subtracted the constant offset of 5 digital counts, are normalized with the incoming irradiance at the top of the atmosphere. Scattered radiation from atmospheric molecules is then subtracted with an empirical expression from Hammer (2000) and the values are then put into bins for each 5th degree of the co-scattering angle ψ. Within each bin the 5, 15, 35, 55, 75, 95 and 98 percentiles are calculated. These percentiles are intentionally representing increasing cloud thickness and/or amounts, provided that the cloud properties are independent of the sun-ground-satellite geometry. The 5 percentile is probably for cloud free cases, and is therefore representative of the ground reflectance. Since the Meteosat data are not calibrated, only the relative variation with geometry will be compared with the corresponding variation of the SHDOM results. Therefore the reflectances are divided by the value of the bin $0º < \psi < 5º$ for each percentile. These normalised reflectances are plotted versus ψ on Figure 5 (solid lines).

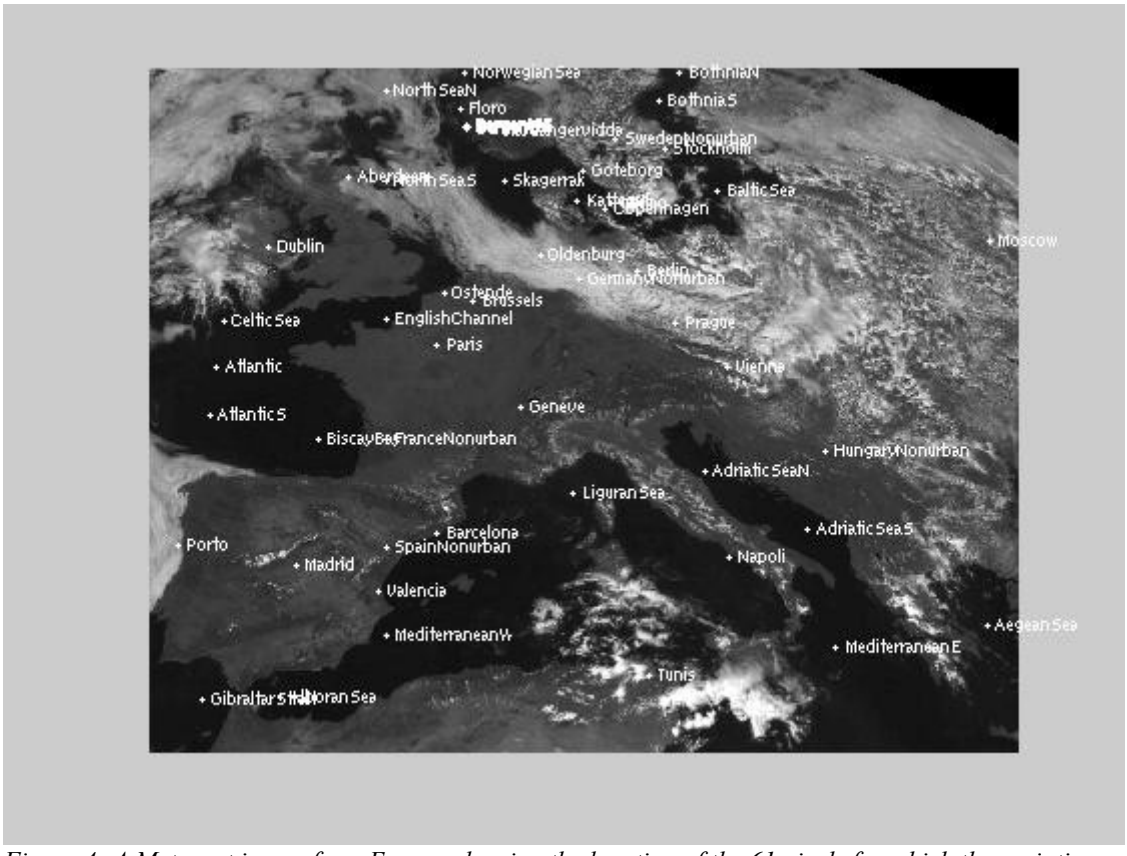

Figure 4: A Meteosat image from Europe showing the location of the 61 pixels for which the variation of bidirectional reflectance has been investigated.

4.2.2 Bidirectional reflectance simulated with SHDOM

Only the stratocumulus cloud field (Figure 1a) is used for this section. The setup of the simulations is identical to the description in section 4.1.1, but more view angles are used: For each of the solar zenith angles, radiance is calculated for every 5th degree of the view zenith angle from 0 to 85 degrees and every 15th degree of the view azimuth angle from 0 to 360 degrees.

The cloud field was not rotated in the azimuth direction, and only the mean radiance from the whole cloud field was used. Since the incoming irradiance at the top of the cloud field is one unit on a horizontal plane, the radiances are equivalent to bidirectional reflectances. The solid line with the black dots on Figure 5 is the mean radiance calculated within the same bins of the co-scattering angle as for the Meteosat-data. Like for the Meteosat data, the simulated reflectances have also been normalised with the mean value for ψ less than 5 degrees, so that only the relative variation of reflectance with ψ is shown.

4.2.3 Comparison of the bidirectional reflectances

Figure 5 shows that the various percentiles of the normalised bidirectional reflectances from Meteosat (solid lines) have a local maximum for ψ below 5 degrees. Then they decrease with ψ until approximately 70 degrees, from where the reflectance is increasing. The variation with ψ is largest for cases with little or no clouds; for thicker clouds (75 and 95 percentiles) the reflectance is close to lambertian. The 98 percentiles of the reflectances are, however, increasing very much when ψ is larger than 30 degrees. Hence in some rare cases the reflectance measured from Meteosat can deviate strongly from lambertian distribution also for very thick clouds.

The normalised radiances from SHDOM (solid line with black dots on Figure 5) have a variation with ψ which is similar to the 15-percentile of the Meteosat-reflectances. However, the simulated radiances increase faster with ψ than the Meteosat-reflectances when ψ is larger than 70 degrees. One of the purposes of this study was to fit a one-parameter (ψ) function to the SHDOM-radiances to be used as a Bidirectional Reflectance Distribution Function (BRDF) for the maximum cloud reflectance in the Heliosat-scheme. However, it appears that the stratocumulus cloud field is too thin to represent the variation of reflectance with the geometry of a thick cloud cover. From the percentile-plots of the Meteosat-reflectances shown on Figure 5 it is also seen that the angular variation of reflectance is larger for low and intermediate cloudiness than for the thickest clouds.

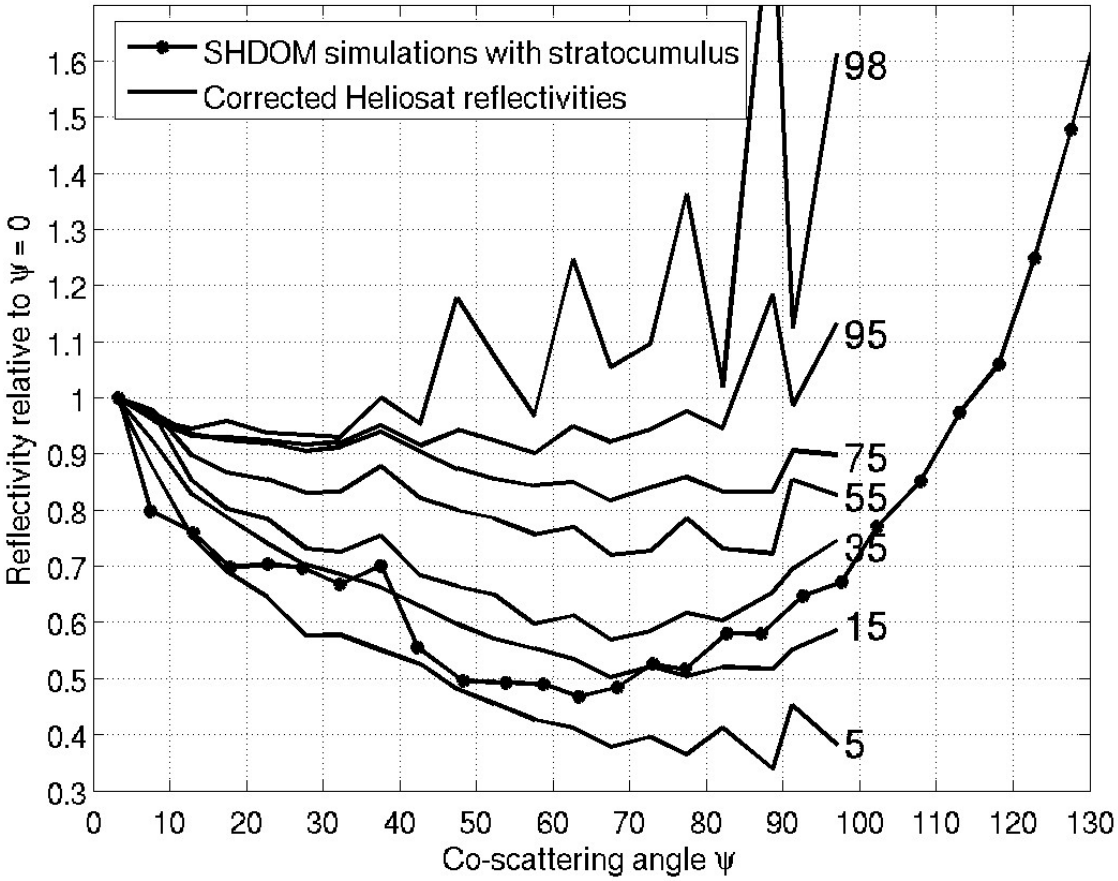

Figure 5: Relative variation of the reflectance of clouds versus the co-scattering angle ψ. The line with dots is the reflectance of a stratocumulus cloud field (Figure 1) calculated with SHDOM (section 4.2.2). The lines without dots are various percentiles of the reflectances measured with the Meteosat HRV sensor for 1996 (section 4.2.1). Each line is labelled with the corresponding percentile number. Both the simulated and observed reflectances are normalised with the corresponding mean value for ψ less than 5 degrees.

5 Summary and conclusions

The variability of bidirectional reflectance of clouds due to 3-dimensional inhomogeneities has been investigated with the 3-dimensional radiative transfer model SHDOM. For very small subsets (~50 metres) of larger cloud fields, there is significant variability of reflectance when the cloud fields are rotated in the azimuth direction. For larger pixel sizes there is a smoothing due to bright and shaded parts cancelling each other. For an overcast stratocumulus cloud field there is almost no variation in the reflectance due to the rotation for a cloud field of the size of 3520 metres. For a broken cumulus field there is some variability (~10-20 %) even for a cloud field at the size of 6700 metres. Hence, for the Heliosat method, averaging reflectances over an area of ~10 kilometres will avoid most variability due to cloud inhomogeneities.

The angular variation of bidirectional reflectance from clouds has also been investigated using both simulations with the stratocumulus cloud field and measurements from the High Resolution Visible channel of the Meteosat satellite. It is found that the simulated reflectances show large variations with the angle between the directions towards the sun and satellite (ψ). The variation is similar to the variation for thin clouds observed by Meteosat. For the thicker clouds, the Meteosat-reflectances are close to lambertian. Hence, the assumption in the Heliosat method of lambertian reflectance from the thickest clouds is reasonable. However, the reflectance varies more with ψ for intermediate cloudiness, so if possible a correction should be made for this in the future.

References

Cano D; Monget JM;, Albuisson M; Guillard H; Regas N; Wald L; (1986) A method for the determination of the global solar radiation from meteorological satellite data, Solar Energy, 37, 31-39

Beyer H.G.; Costanzo C.; Heinemann D; (1996) Modifications of the heliosat procedure for irradiance estimates from satellite images, Solar Energy, 56, 207-212

Fontoynont, M; Dumortier, D; Heinemann, D; Hammer, A; Olseth, J A; Skartveit; Ineichen, P; Reise, C; Page, J; Roche, J; Beyer, H; Wald, L (1998) Satel-Light: A www server which provides high quality daylight and solar radiation data for western and central Europe,

Rigollier, C; Lefèvre, M; Wald, L (2004) The method Heliosat-2 for deriving shortwave solar radiation from satellite images, Solar Energy, 77, 159-169

Evans, K. F (1998) The spherical harmonic discrete ordinate method for three-dimensional atmospheric radiative transfer, J. Atmos. Sci., 55, 429-446

Moeng, C.-H., W. R. Cotton, C. Bretherton, A. Chlond, M. Khairoutdinov,S. Krueger, W. S. Lewellen, M. K. MacVean, J. R.M. Pasquier, H. A. Rand, A. P. Siebesma, B. Stevens, and R. I.Sykes, (1996) Simulations of a stratocumulus-topped planetary boundary layer: Intercomparison among different numerical codes, Bull. Amer. Meteor. Soc., 40, 51-69

Hammer, A (2000) Anwendungsspezifische Solarstrahlungsinformationen aus Meteosat-daten, PhD thesis, University of Oldenburg